

Longitudinal Distribution of suprathermals and SEPs -- New Insights from ACE, Wind, and STEREO

Feb 2009, STEREO-SWG, Pasadena, CA

M. I. Desai

Southwest Research Institute, San Antonio, TX, USA

Team Members

Name	Institution	Role/Responsibility
Mihir Desai	SwRI	PI - Particle Data from STEREO, ACE, Wind
Heather Elliott	SwRI	Col, Solar Wind Data from ACE & Wind
Frederic Allegrini	SwRI	Col - Particle Data from STEREO, ACE, Wind
Maher Al-Dayeh	SwRI	Postdoc - Particle Data from STEREO, ACE, Wind
Mark Popecki	UNH	Co-I; Solar wind from STEREO
Gang Li	UAH	Co-I; - Modeling of SEPs
Rick Leske	Caltech	High-energy data from STEREO & ACE
Gary Zank	UAH	Collaborator: Modeling
Glenn Mason	JHU/APL	Collaborator: Low--energy particle data from Wind, STEREO & ACE
Dick Mewaldt	Caltech	Collaborator: High-energy data from STEREO & ACE

Outline

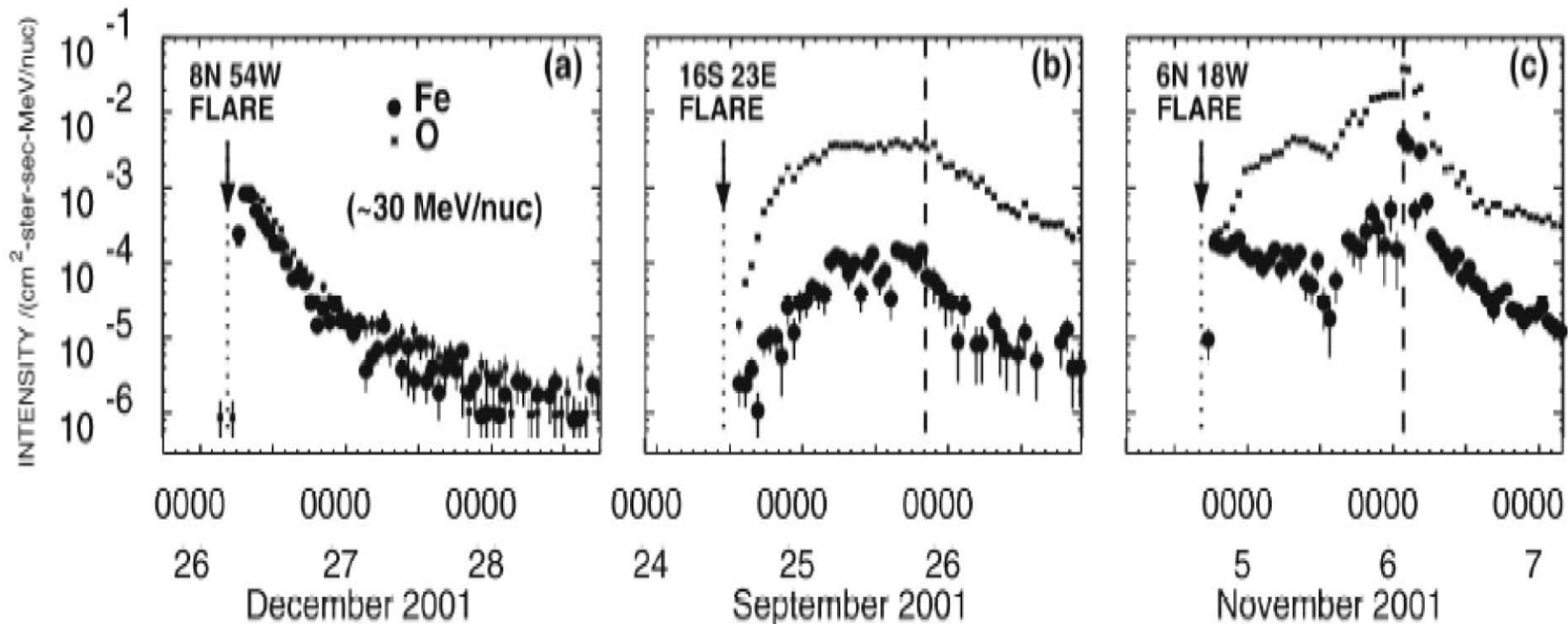
- Overview
- Goal & Approach
- Status of Proposed Work
 - EP & Magnetic field Data
 - Suprathermal ion & solar wind data
 - 2D Modeling using Helios 1 & 2, and IMP-8
 - Overall Project Status
- Other STEREO-related Science Projects

Cane et al., 2003; 2006

**Western events:
High Fe/O =>
direct Flare
population**

**Eastern events:
Fe/O < 0.2 =>
Shock-accelerated
population**

**Central Meridian
Events: High Fe/O
followed by lower
Fe/O at shock =
Flare+shock**

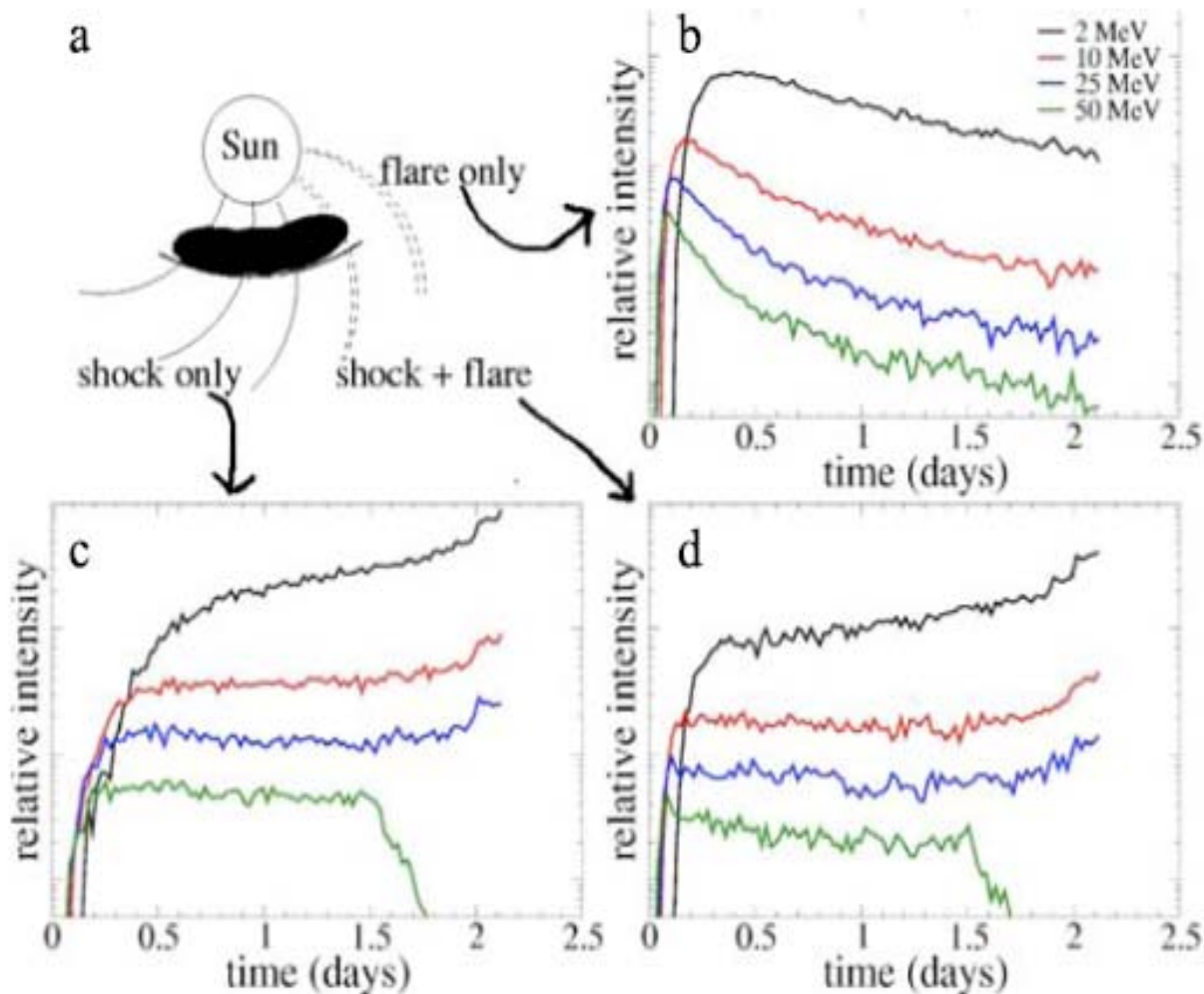




SEP properties (time profiles, Fe/O ratio, anisotropy etc) depend on the location of s/c relative to flare location

QuickTime™ and a
TIFF (Uncompressed) decompressor
are needed to see this picture.

Li & Zank - 1D model



Time-profiles depend on the relative location of flare site to observer

Western -- flare only

Central Meridian -- flare + shock

Eastern -- shock only

Causes of longitudinal Variability

- Interplanetary conditions e.g., CMEs and/or CME interactions (Cane et al., 2006; Gopalswamy et al. 2005)
- Seed population variability (Desai et al, 2006)
 - SW vs availability of suprathermals
- Shock obliquity (Tylka & Lee 2006)
 - Quasi-parallel vs quasi-perpendicular injection & acceleration
- Direct Flare Contributions (Cane et al., 2003)
- Particle scattering in the IP Medium (Mason et al. 2006)

Objective

Evaluate the relative importance of interplanetary conditions, the suprathermal seed population, shock injection and acceleration, and particle scattering in driving the longitudinal dependence of SEP properties observed at 1 AU



100,000,000, Wind + 20 Modeling of cycle 24 SEP

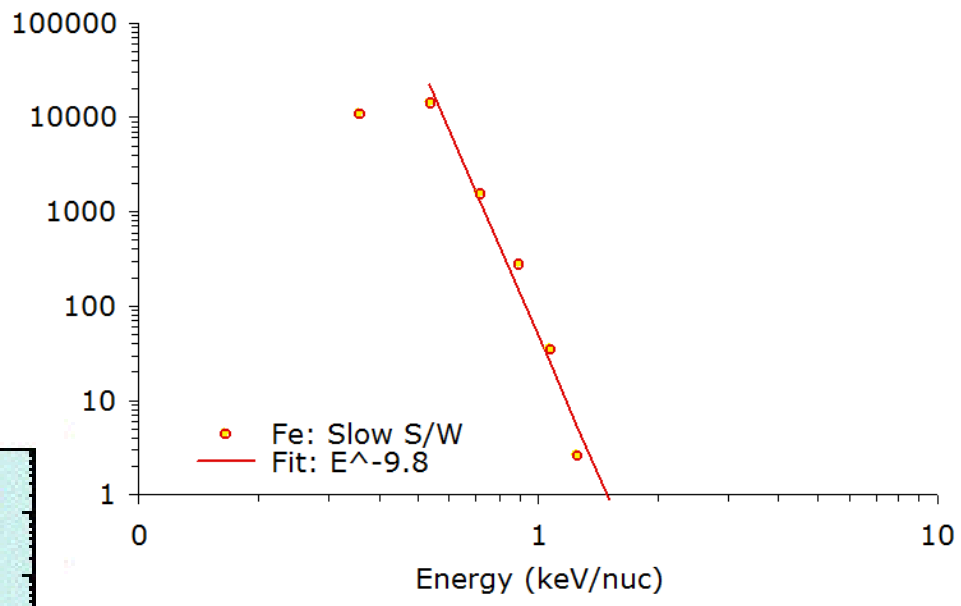
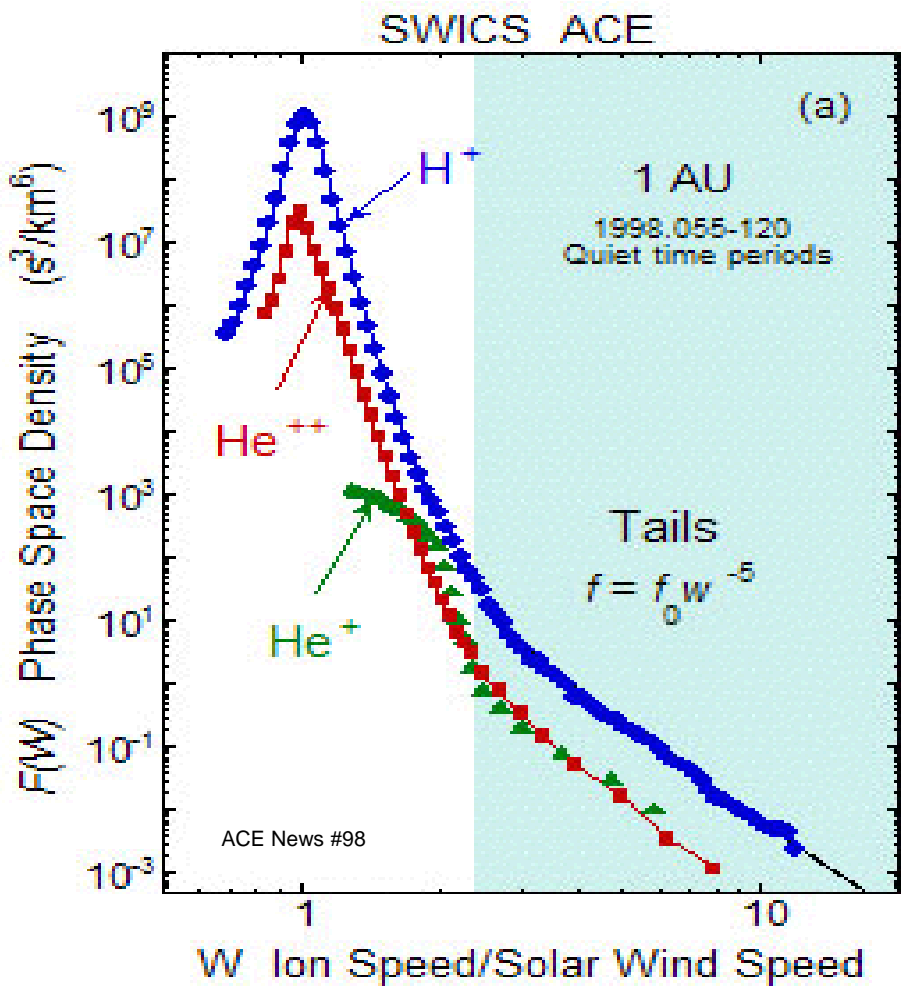
QuickTime™ and a
TIFF (Uncompressed) decompressor
are needed to see this picture.

- 1. Flare contributions - direct vs seed population?**
- 2. Role of variable seed populations and their injection mechanisms at shocks with different obliquity?**
- 3. Effects of rigidity-dependent scattering during acceleration, escape, and transport?**

Years 1 & 2 -- Goals and Progress

- Create EP and mag field data analysis tools
 - ➔ Automated routines for data download and processing -- assisted by Glenn Mason & Andy Davis
- PLASTIC SW and suprathermal data analysis
 - ➔ In progress
- Develop 2D Model to simulate SEPs from previous solar cycle
 - ➔ In Progress
- Data analysis and modeling of SEPs as they occur in cycle 24

Energy Spectrum of Solar Wind Fe



- Power-law exponent for Fe is steeper than that predicted by Fisk and Gloeckler et al.
- H and He observations (Figure 1), which is located at lower speeds than the $E^{-1.5}$ suprathermal tail region.

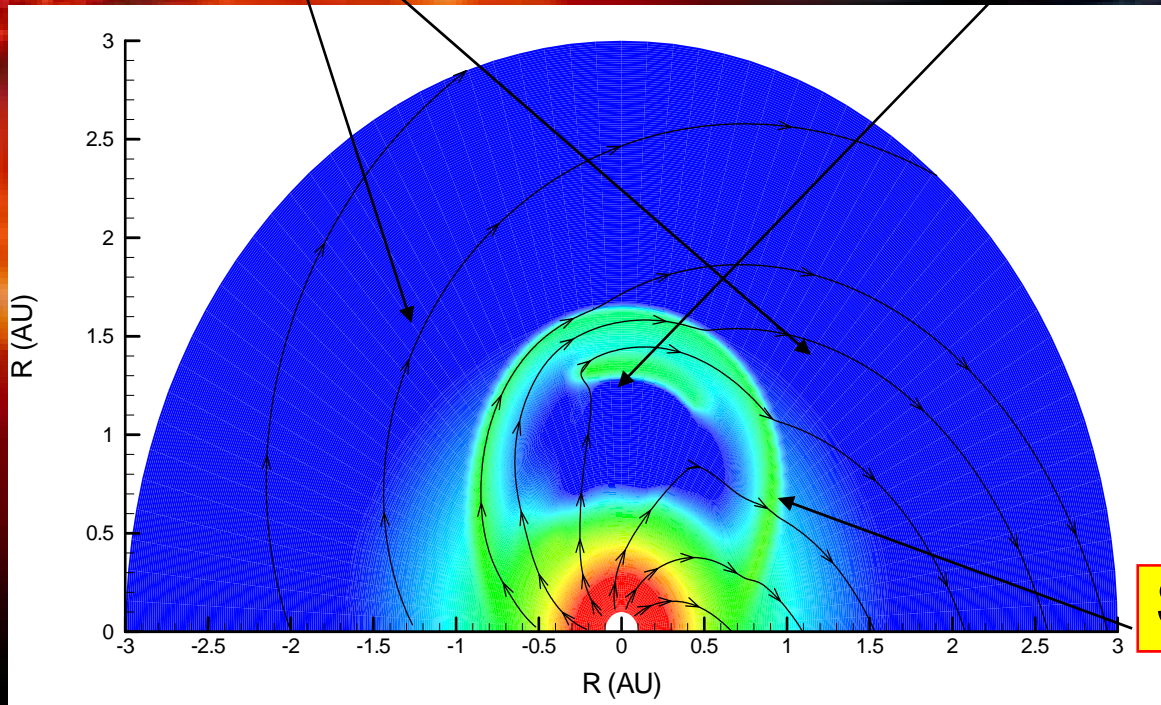
Two-dimensional model

Magnetic field lines

Ejecta

Shock geometry varies along the shock front =>

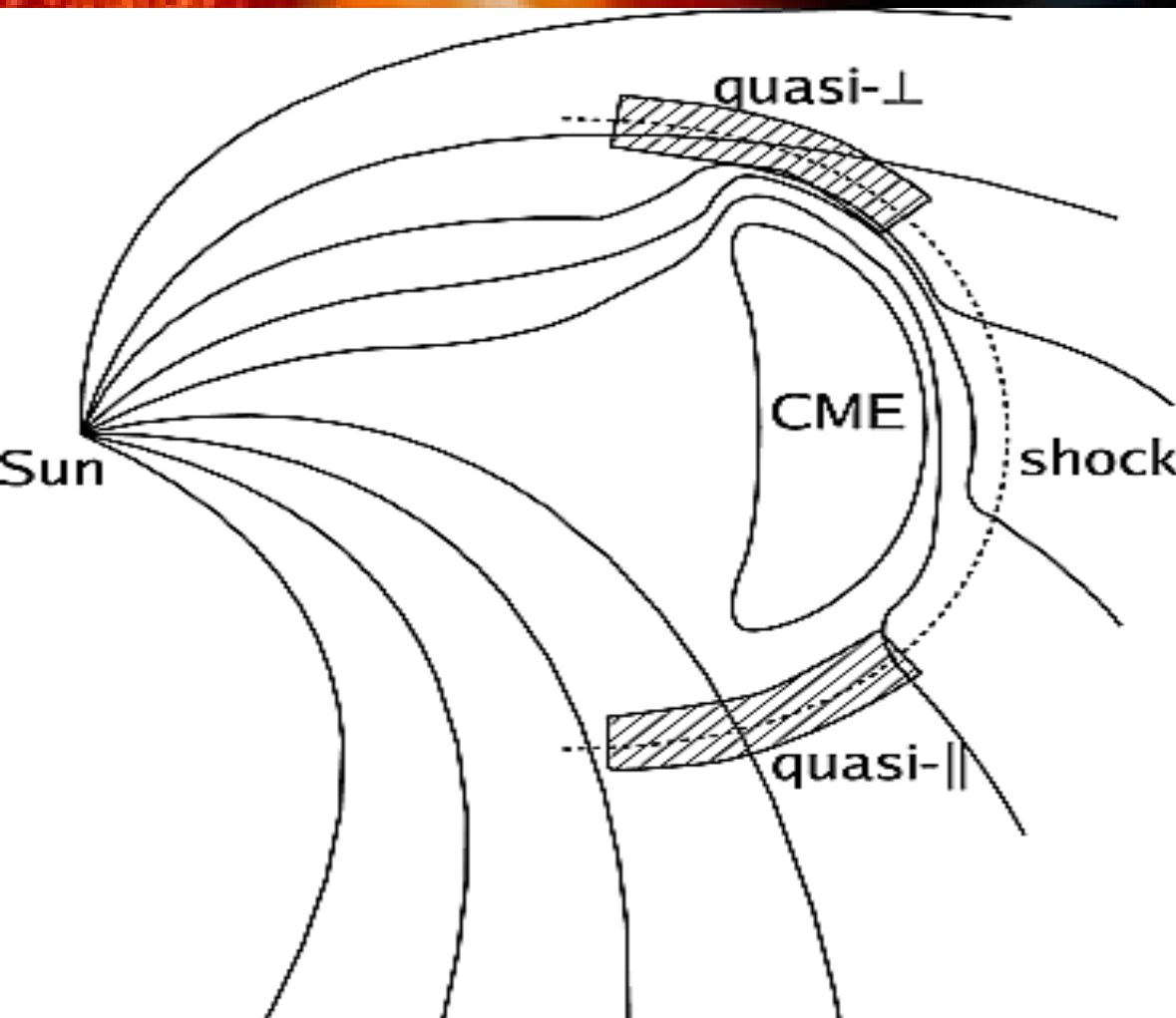
2D simulation is needed



Shock front

- A two dimensional MHD code will be used to simulate the coronal mass ejection driven shock.

Acceleration at an oblique shock

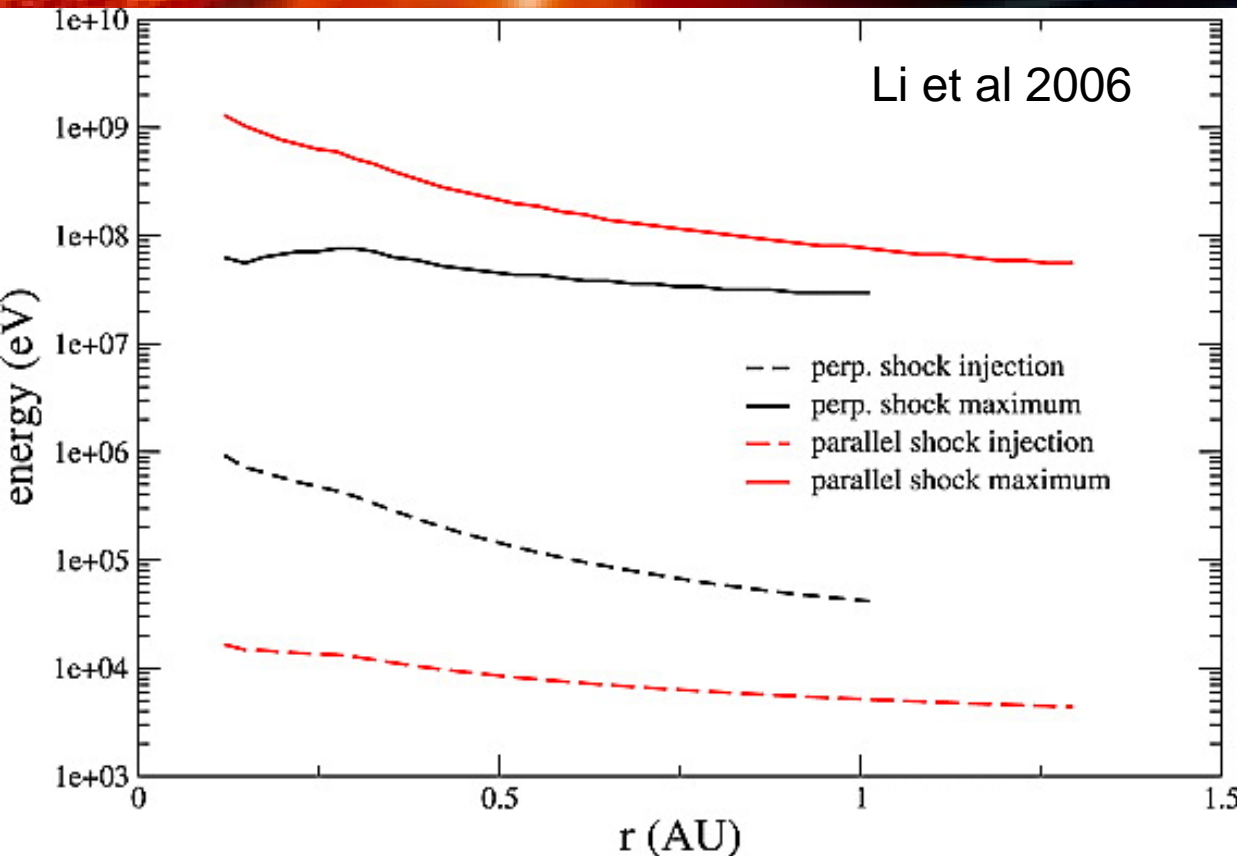


CME shock is dynamic – evolving with time and changing geometry along the shock surface.

Acceleration needs to consider the effect of κ_{\perp} , which differs from quasi-parallel shock

This is further tangled with transport (field line jumping)

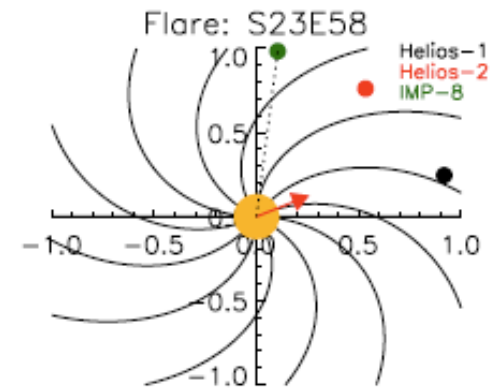
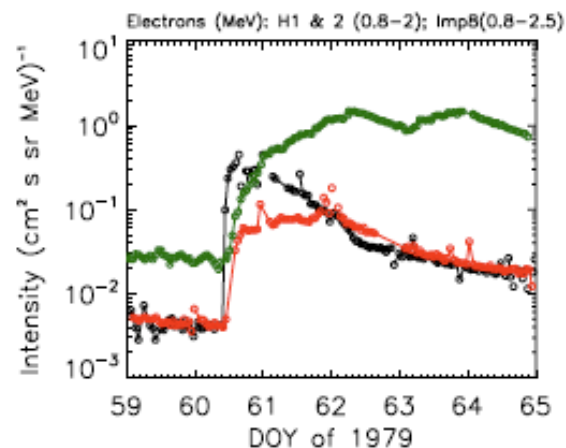
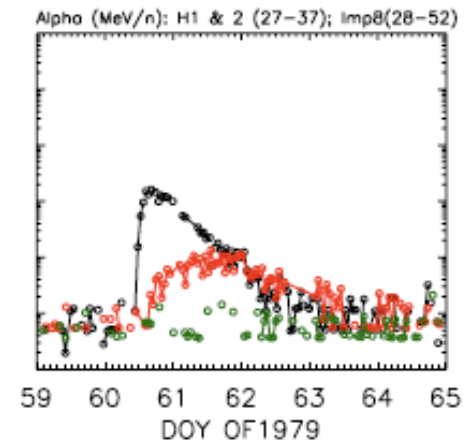
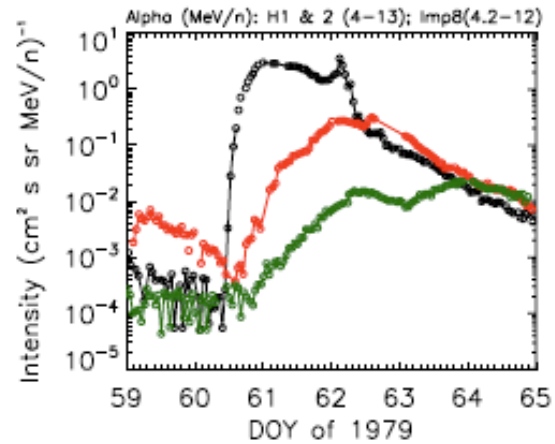
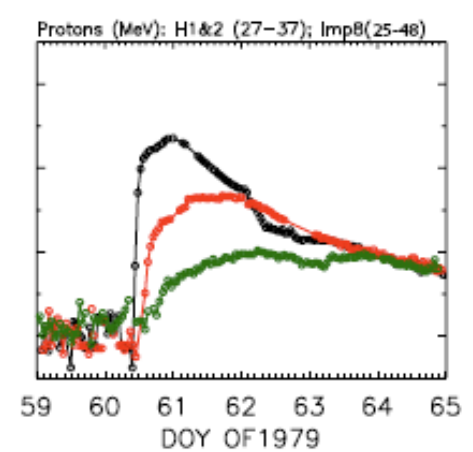
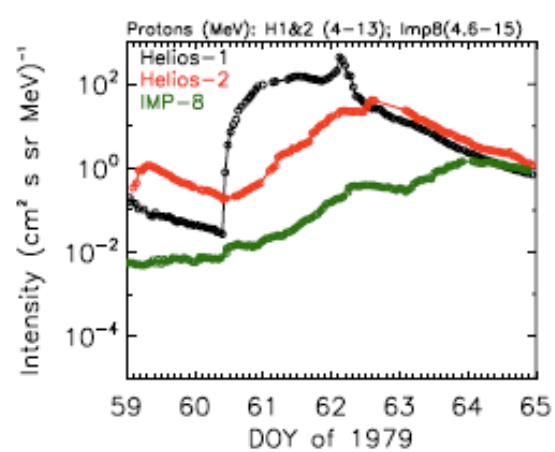
Preliminary results: Maximum energy for quasi-parallel and quasi-perp. shocks



- Ignore change of shock geometry during shock propagation.
- Consider a parallel shock and a quasi-perp. Shock (85 degree).
- Parallel with a strong turbulence reaches a higher energy than a quasi-perp shock.
- Perp. shock requires higher injection

Cycle 22 SEPs

- Use plasma, magnetic field, and particle data at Helios 1, 2 and IMP-8 for developing and validating the 2D model
- In the process of modeling 2 SEP events

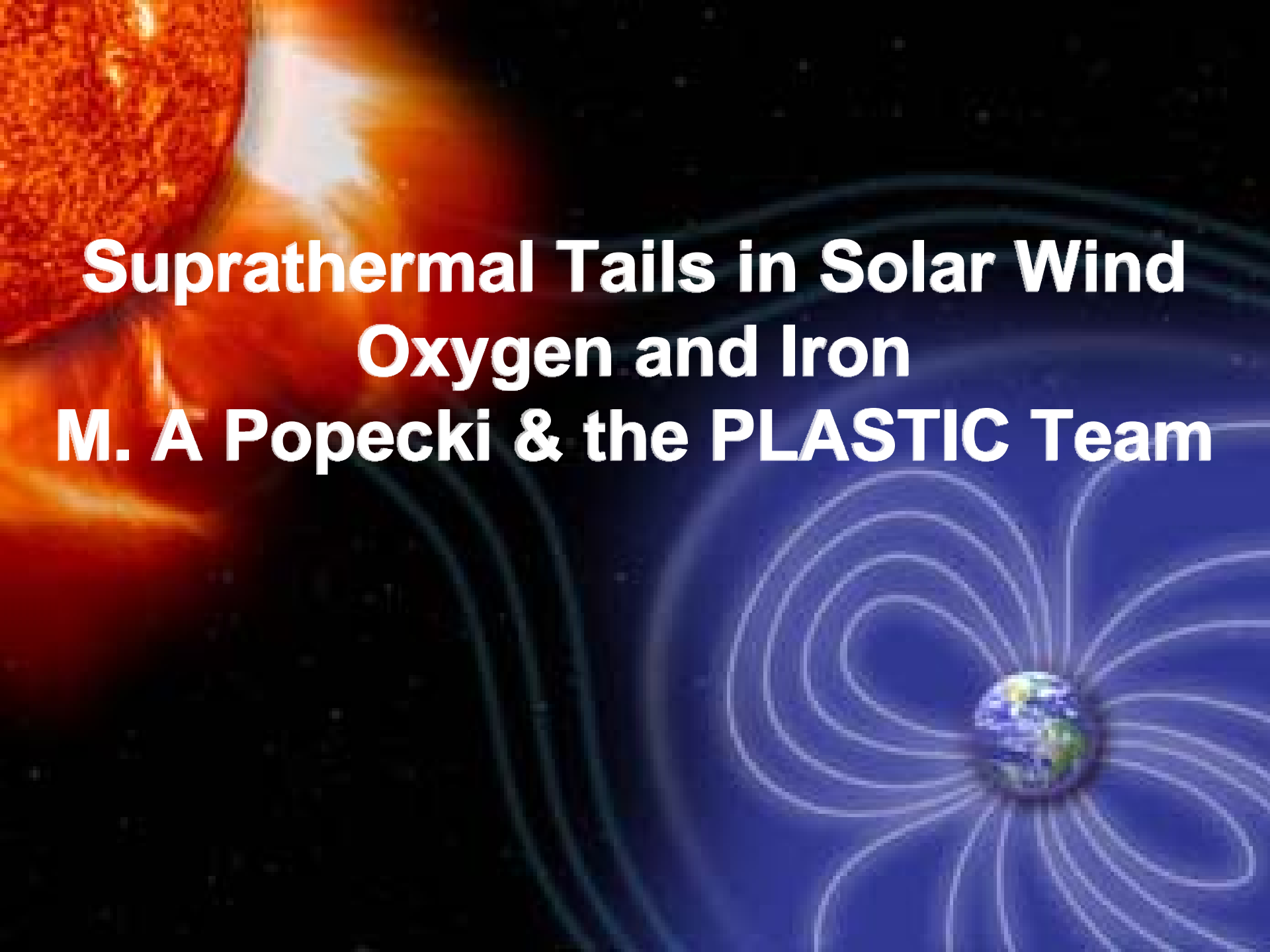


Summary

- Like the rest of the STEREO Team, we are eagerly awaiting the start of solar activity and SEPs
- SEP Data Analysis and Modeling work in good shape --- expect results in Spring & Summer
- Distant Upstream ion events with ACE, Wind & STEREO-A (Desai et al., 2008)
- CIR properties at ACE & STEREO (Mason et al., 2008; 2009)
- Properties of Suprathermal Tails over a solar cycle (Al-Dayeh et al., 2009)
- CME-shock Accelerated ions over a solar cycle (Allegrini et al., 2009)

The image is a composite graphic. On the left side, there is a large, detailed view of the Sun, showing its bright orange and red surface with solar flares and sunspots. On the right side, there is a smaller Earth globe surrounded by white, glowing magnetic field lines that form a complex, multi-lobed pattern. The background is a dark, starry space. In the center, the words "The End" are written in a bold, white, sans-serif font.

The End

The background of the slide is a composite image. On the left side, there is a close-up, fiery view of the Sun's surface, showing bright orange and red colors with a granular texture. On the right side, there is a depiction of Earth's magnetic field, represented by white, glowing, curved lines that form a complex, multi-lobed pattern around a small, realistic image of the Earth. The overall background is a dark blue gradient.

**Suprathermal Tails in Solar Wind
Oxygen and Iron
M. A Popecki & the PLASTIC Team**

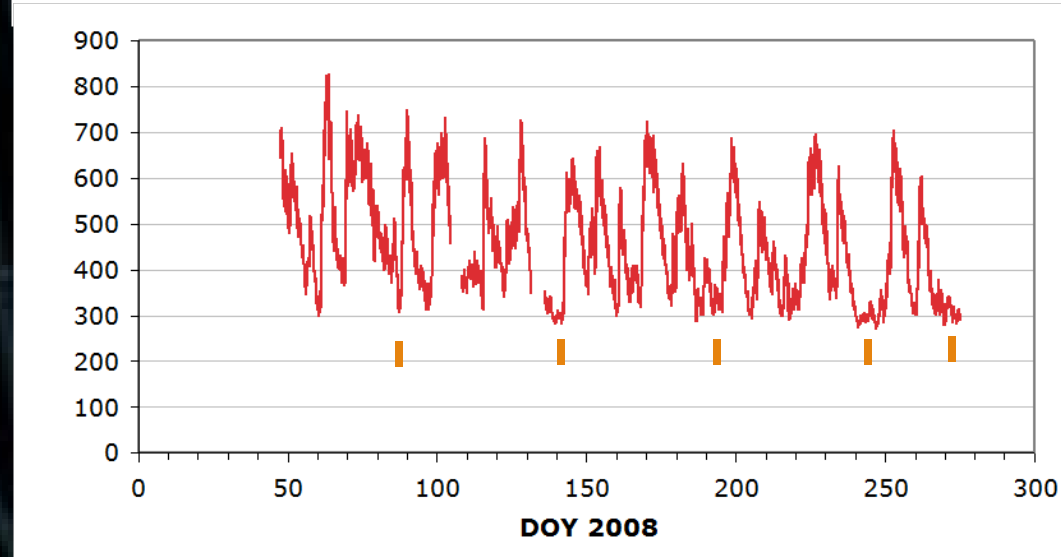
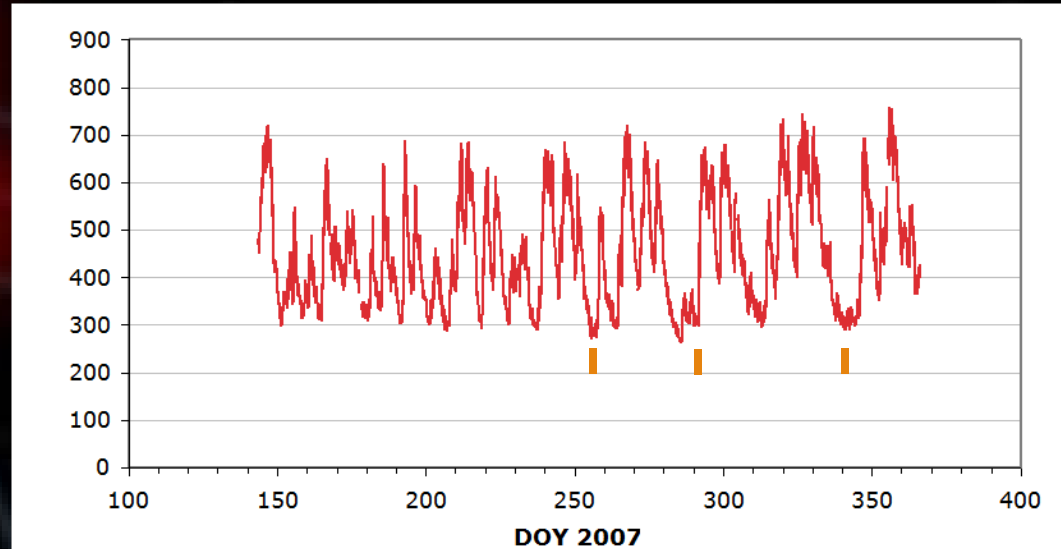
PLASTIC - Suprathermal Ion Studies

Periods with low solar wind speeds allows the highest possible ratio of heavy ion speed to proton speed within the fixed energy limits of the instrument.



High and low speed solar wind selection and calculation of spectra

- Examples of high and low speed solar wind were selected. Selected periods of low speed solar wind are indicated at right with orange bars.
- Counts/(energy/q) step were extracted.
- Charge states were calculated and used to get counts/speed step.
- The energy spectrum of Fe and O were obtained.



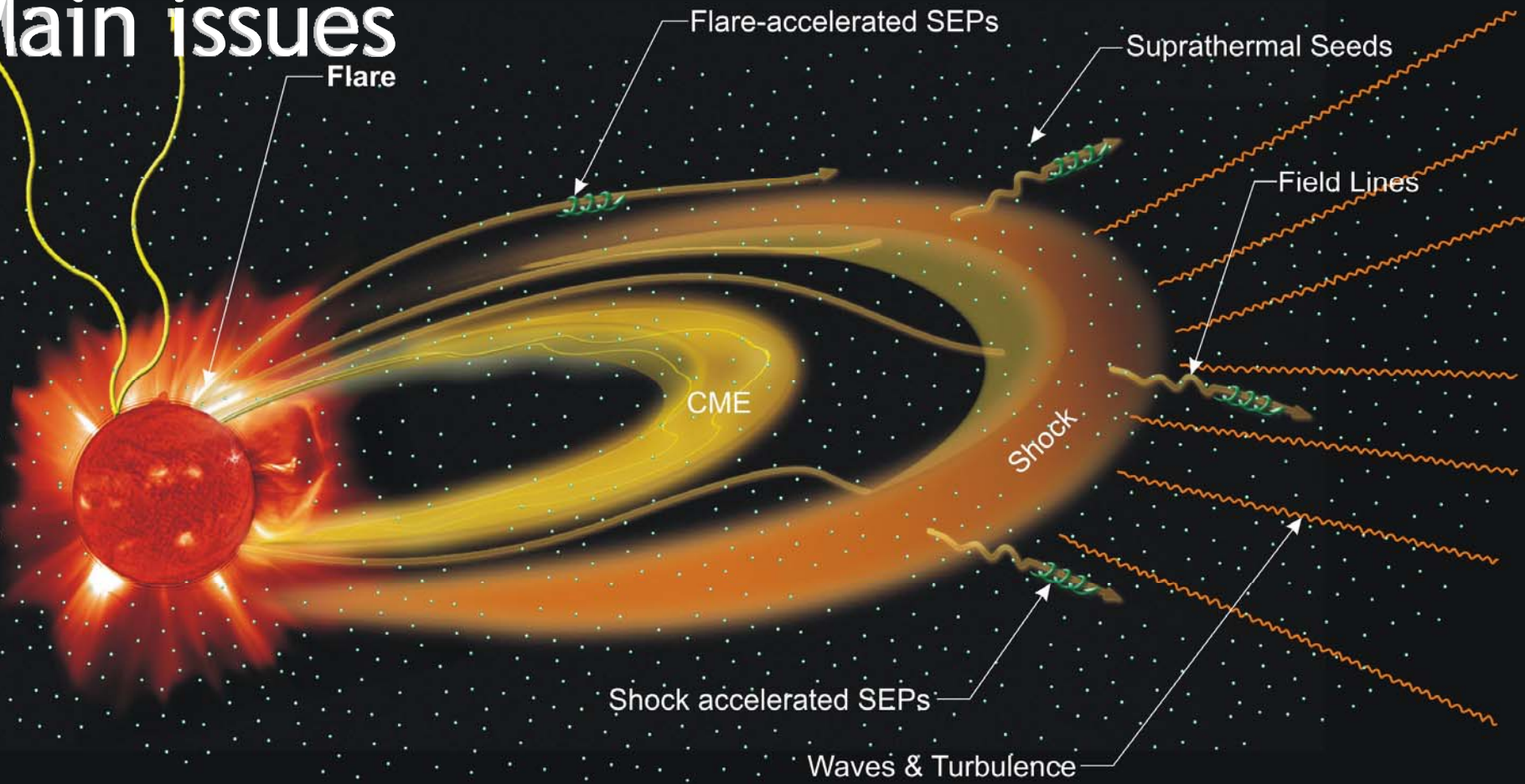
Summary

- The energy spectra of solar wind O and Fe have been calculated for low and high speed periods.
- Both O and Fe count spectra display tails above the H^+ solar wind speed.
- Spectral variations appear in both ion species.
- Ionic charge states decrease with increasing energy in both Fe and O.
- The low speed Fe measurements do not extend up into the E-1.5 suprathermal tail region in which Gloeckler et al. find constant spectral forms (Fig. 1).
- The fluence spectrum of suprathermal Fe for low speed solar wind falls somewhat faster than their H and He observations, up to $V/V_H \sim 1.7$.
- Next: O and C tails may extend to higher speeds in sufficient quantities to examine the spectral form above $V/V_H = 2$.

Programmatics

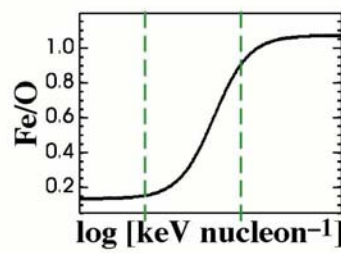
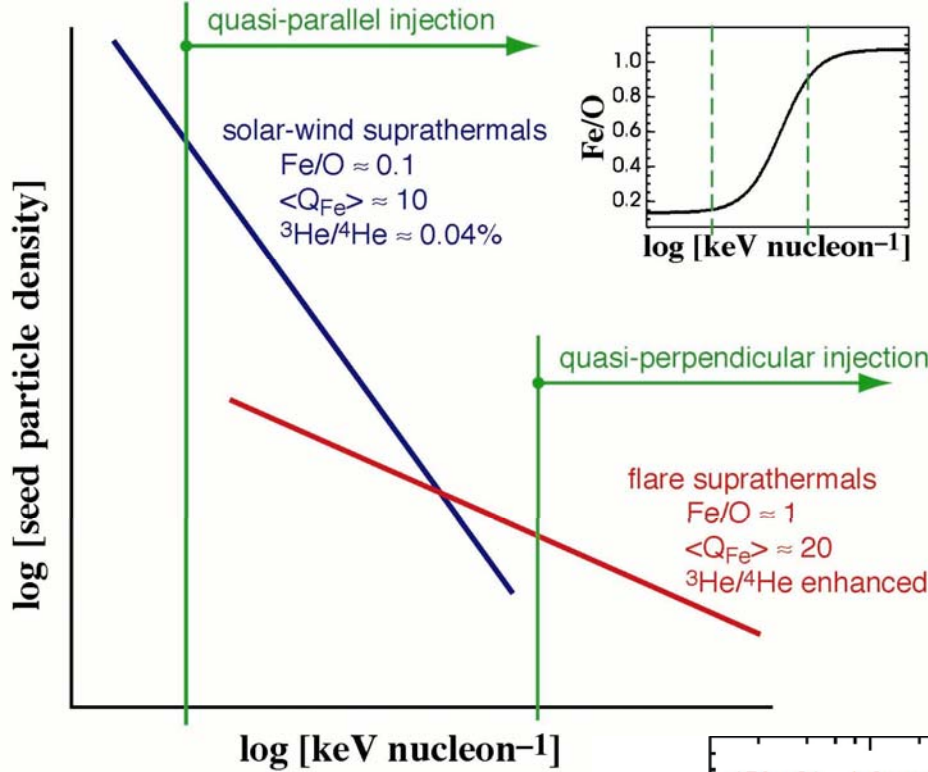
- Monthly team telecons
- Meetings
 - SoHO/STEREO -- Bournemouth England
 - SW 12 - Saint Malo, France
 - ICRC -- Poland
 - Fall AGU -- San Francisco

Main issues



1. Flare contributions - direct vs seed population?
2. Role of variable seed populations and their injection mechanisms at shocks with different obliquity?
3. Effects of rigidity-dependent scattering during acceleration escape and transport?

Tylka & Lee (2005)



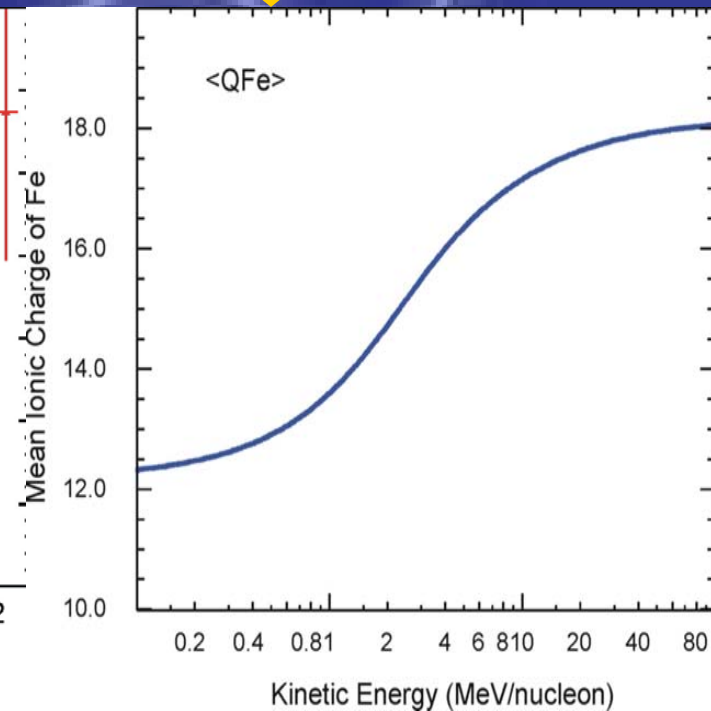
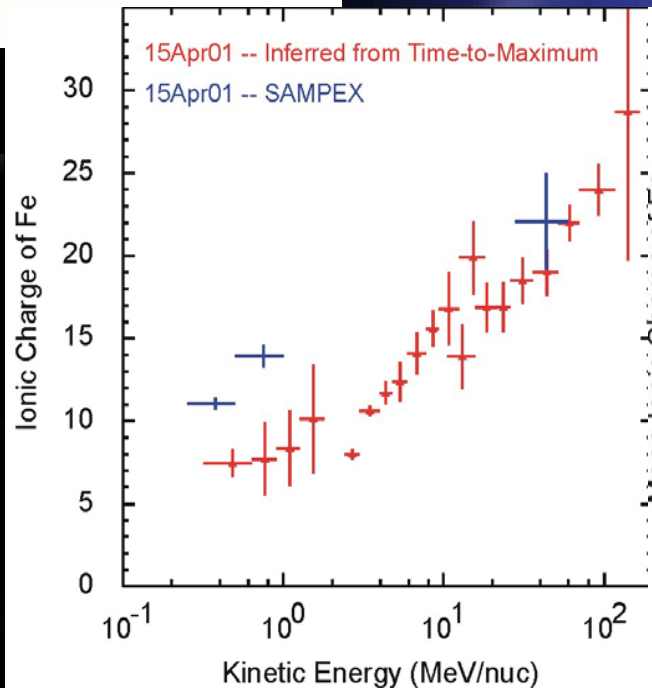
- uses mixture of seed populations
- Shock geometry is critical
- Produces increasing Fe/O with energy and positive correlation of high Q state and Fe/O

Tylka et al., ApJ 2005

SAMPEX: Labrador et al. (2003)

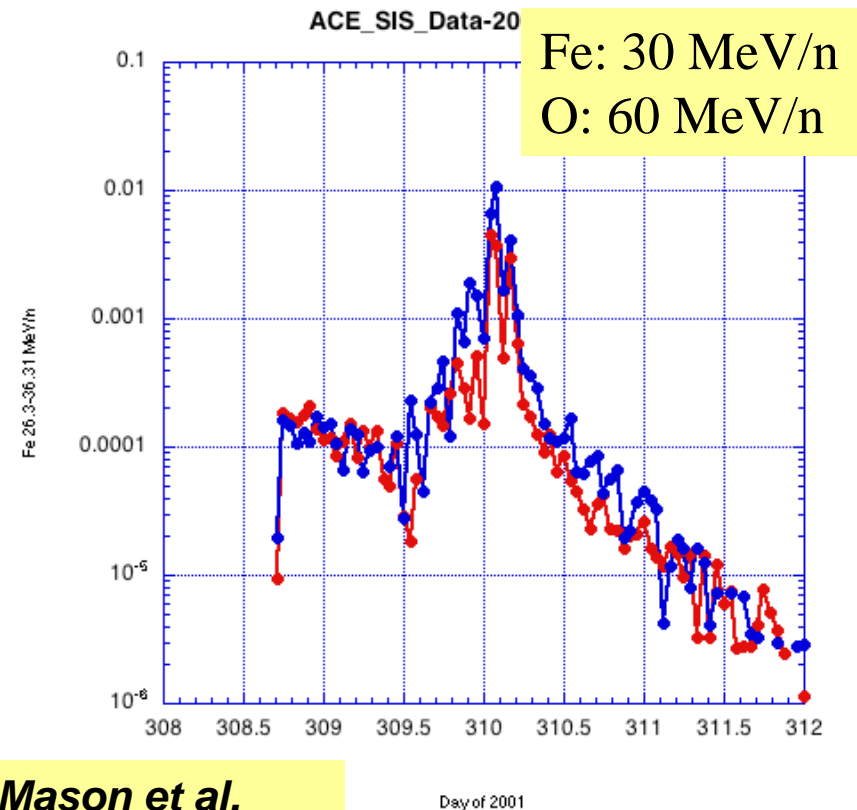
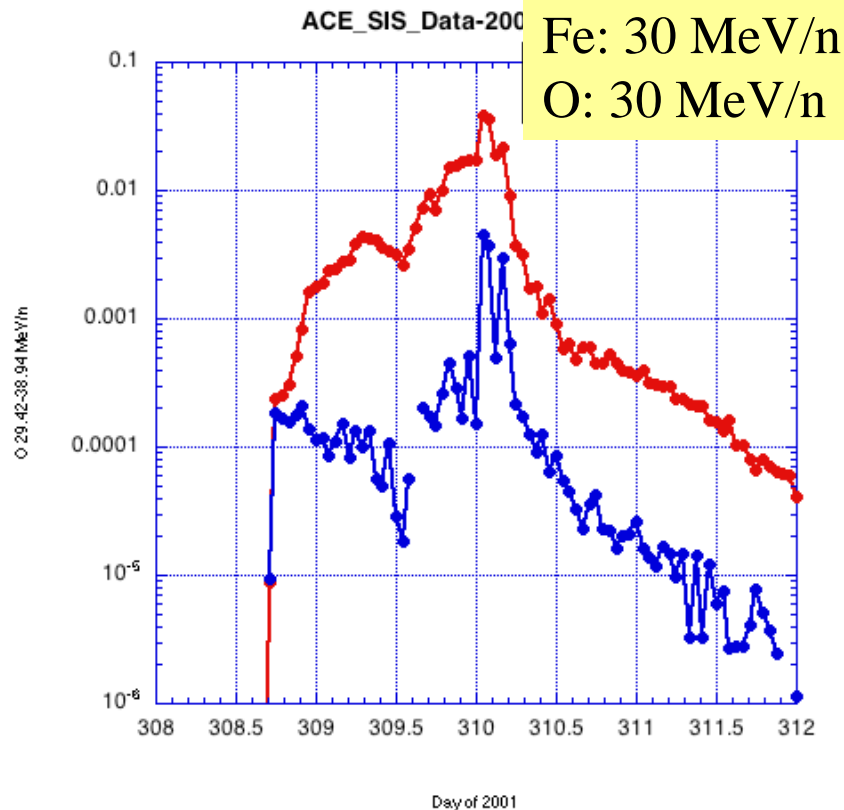
Mazur, private communication.

TTM: Dietrich & Tylka 2003



November 4, 2001 --- **only one interplanetary scattering dominated component (Mason et al. 2006)**

Time-profiles at same rigidity

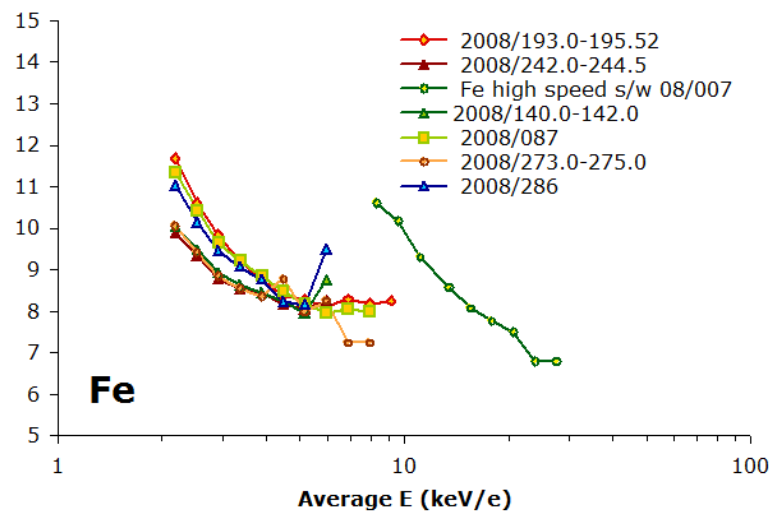
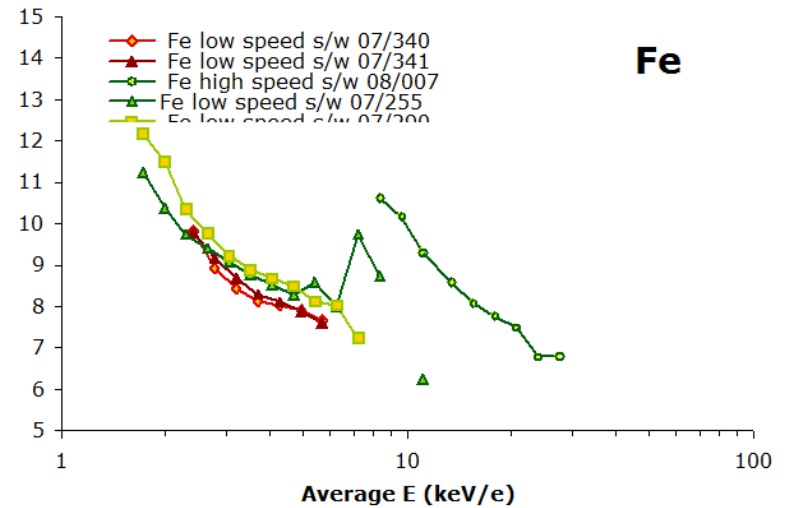
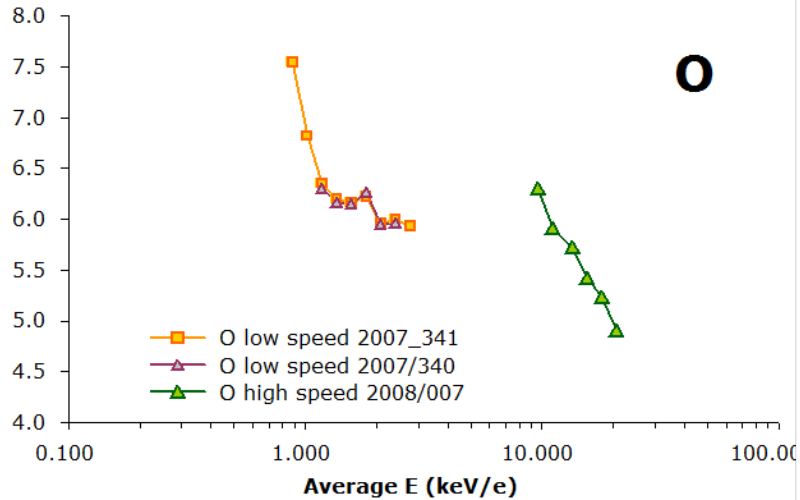


Mason et al.
2006

O, Fe At same MeV/n

O has ~twice the kinetic energy as Fe

Q(E) for high and low speed O and Fe

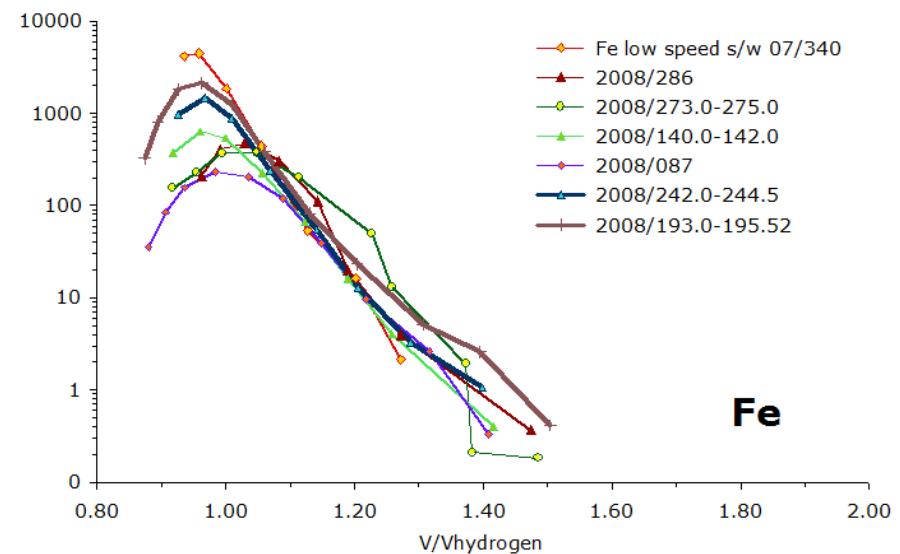
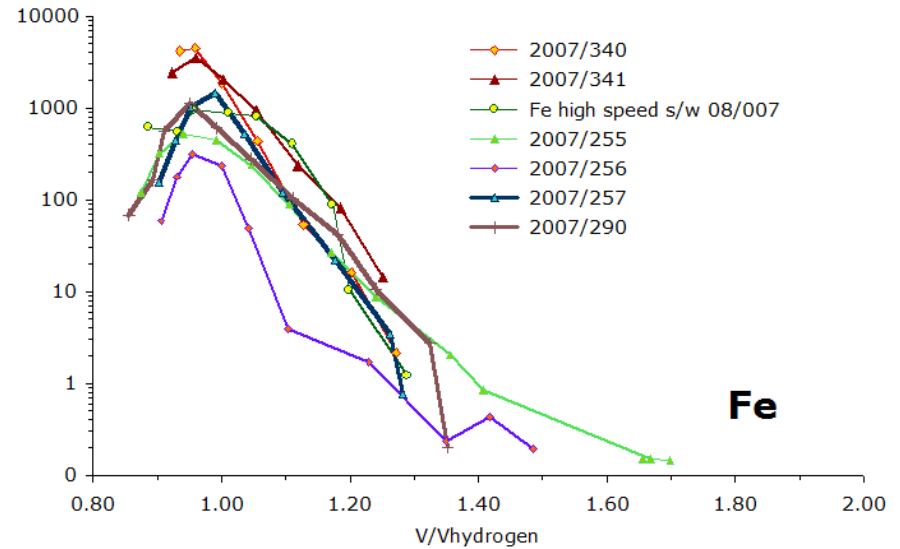


- Average charge states are shown for each ESA step range: Q(E).
- Charge states tend to decrease with increasing energy.
- The charge states and ESA step energies together provide the average energies.



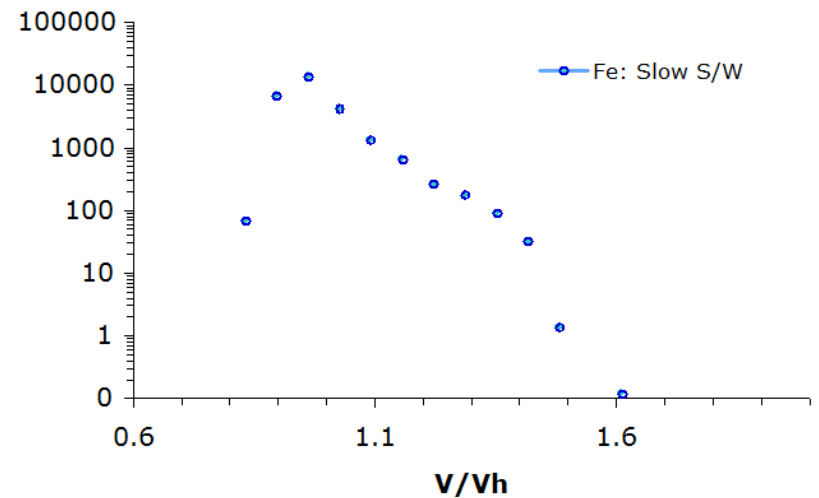
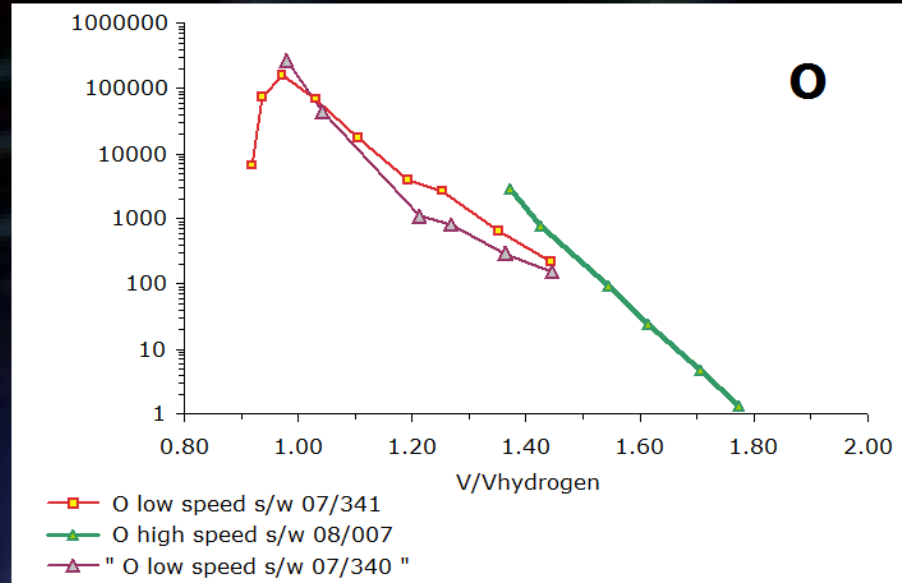
Spectra in V/V_H

- Spectra are shown for Fe as a function of speed relative to solar wind H.
- Most events are from low speed solar wind (~ 300 km/s) periods.



Counts/keV vs. V/V_H

- Top: Fe and O counts/keV vs. S/W speed ratio are shown.
 - Individual events are shown for O
- Bottom: All low speed solar wind Fe events in are integrated into a single fluence spectrum.
 - ✓ A peak is present near $V/V_H = 1$, then a shoulder in the spectrum develops at higher speeds.
 - ✓ However, Fe is not measured at speed ratios beyond 1.7. This is limited by the instrument geometric factor and pulse height data download limits. The limit of ~ 1.7 is insufficient to compare to the tails in Gloeckler et al. H and He measurements of constant spectral form above $V/V_H \sim 2$.



κ in perpendicular shocks - NLGC theory

At a quasi-perp. shock, Alfvén wave intensity goes to zero, so contribution of $\kappa_{\parallel} \cos(\theta)$ can be ignored. The major contribution comes from κ_{\perp} .

Need a good theory of κ_{\perp}

Simple QLT:

$$\kappa_{\perp} = \kappa_{\parallel} / [1 + (\lambda_{\parallel} / r_l)^2]$$

Jokipii 1987

Non-linear-Guiding-center:

$$\kappa_{\perp} = \frac{a^2 v^2}{3B^2} \int_0^{\infty} \frac{S_{\perp}(\mathbf{k}) d^3 \mathbf{k}}{v/\lambda_{\parallel} + k_{\perp}^2 \kappa_{\perp} + k_{\parallel}^2 \kappa_{\parallel}}$$

Matthaeus et al 2003

$$\lambda_{xx} \approx (\sqrt{3}\pi a^2 C)^{2/3} \left(\frac{\langle b_{2D}^2 \rangle}{B_0^2} \right)^{2/3} \lambda_{2D}^{2/3} \lambda_{\square}^{1/3} \left[1 + \frac{(a^2 C)^{1/3}}{(\sqrt{3}\pi)^{2/3}} \frac{\langle b_{slab}^2 \rangle}{\langle b_{2D}^2 \rangle^{2/3} (B_0^2)^{1/3}} \frac{\min(\lambda_{slab}, \lambda_{\square}/\sqrt{3})}{\lambda_{slab}^{2/3} \lambda_{\square}^{1/3}} \left(4.33H(\lambda_{slab} - \lambda_{\square}/\sqrt{3}) + 3.091H(\lambda_{\square}/\sqrt{3} - \lambda_{slab}) \right) \right]^{-2/3}$$

Zank et al 2004

Suprathermal Tails in H & He

- High speed tails have been observed in solar wind H⁺ and He⁺⁺, as well as in pickup He⁺ (Gloeckler, Gloeckler & Mason; see ACE News #98).
- Tails have implications for particle injection into the shock acceleration process.
- Above speeds of $\sim 2V_{sw}$, the tails appear to have a constant profile regardless of solar wind conditions.
- The slope goes as $(V_{ion}/V_{s/w})^{-5}$ in phase space density, and as $E^{-1.5}$ in energy.
- We will investigate heavy ion speeds and characterize possible tails in ions heavier than He.
- Using STEREO/PLASTIC:
 - The energy spectrum of O and Fe may be obtained from periods of high and low speed solar wind.

